Reaction Mechanism of an Intramolecular Oxime Transfer Reaction: A Computational Study

Jani Moilanen,* Antti Neuvonen, Petri Pihko*

Department of Chemistry, University of Jyväskylä, P.O. Box 35, FI-40014 Jyväskylä, Finland

* jani.o.moilanen@jyu.fi; petri.m.pihko@jyu.fi

Table of Contents

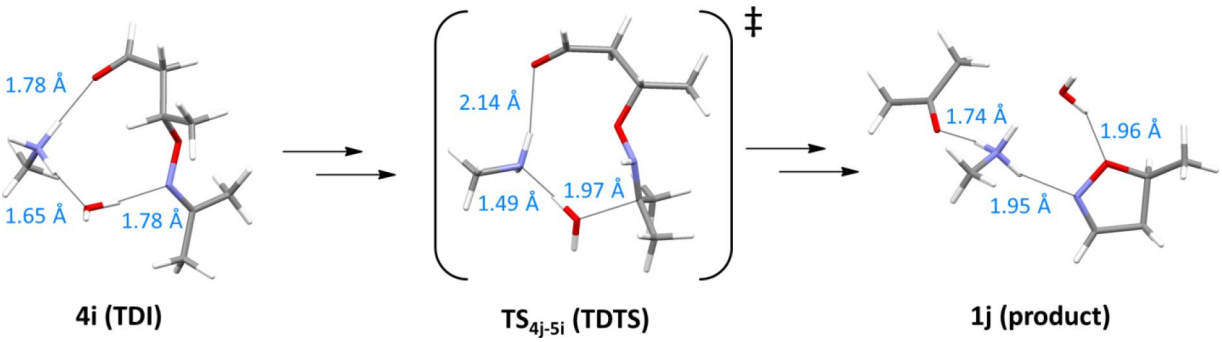

Abstract

Density functional theory (PBE0/def2-TZVPP) calculations in conjunction with polarizable continuum model were used to assess the reaction mechanism of intramolecular oxime transfer reaction that leads to the formation of isoxazolines. Different diastereomers of the intermediates as well as different oximes (formaldehyde and acetone oxime) were considered. The computed reaction profile predicts the water addition and expulsion steps as the highest barriers along the pathway, a conclusion which is in line with the experimental evidence obtained previously for these reactions.

Introduction

Gathering evidence for a proposed reaction mechanism involving several reactive intermediates and complex equilibria can be challenging even with modern spectroscopic methods and kinetic experiments. The main difficulty arises when the intermediates escape experimental detection and identification. In these cases, the use of computational methods should give further insights into the plausibility of the mechanism and the relative stabilities of postulated short-lived intermediates. Herein, we discuss a case involving a seemingly simple oxime transfer reaction where the key intermediates could not be detected experimentally and a tentative mechanism was inferred from substituent effects.

We have previously reported both racemic and enantioselective organocatalytic methods for the synthesis of 3-unsubstituted 2-isoxazolines (**1**) from oximes (**2**) and α,β-unsaturated aldehydes (**3**).[1] In conjunction with these studies, the mechanism of this transformation has been studied by kinetic measurements and analysis of the product distributions, leading to the following observations on the mechanism.[1b] NMR monitoring of the reaction progress indicated that the reaction likely proceeds via the conjugate addition product **4**, since the concentration of this intermediate climbs and falls during the initial stages of the reaction, and the concentration of isoxazoline then starts to increase. Evidence for the iminium catalysis of this step can be obtained from the observed sense of enantioselection when the reaction was carried out with chiral amines (Scheme 1).

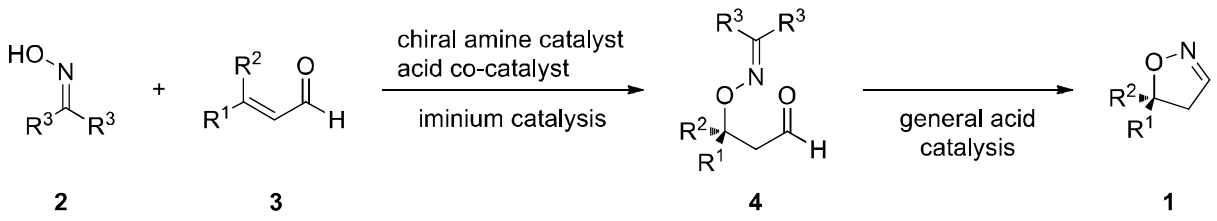

Scheme 1. Previously reported organocatalytic asymmetric synthesis of 2-unsubstituted isoxazolines.

However, less conclusive evidence could be obtained for the mechanism of the oxime transfer reaction in which the conjugate addition product **4** is converted to the isoxazoline **1**. Experimentally, this step was examined by NMR with separately prepared conjugate addition product **4**, and these studies established that this sequence was likely to be acid-catalyzed and not iminium-catalyzed. Faster rates were obtained with acids such as diphenyl phosphate than with the corresponding ammonium salts (e.g. *N*-methylammonium diphenyl phosphate). Further investigations of the entire reaction sequence suggested that increasing the concentration of water in the reaction medium increased the rate slightly, while a further substitution in the β position of the enal **3** led to more significant increases in the overall rate and concomitant decrease in the peak concentration of the intermediate **4**. Furthermore, cyclohexanone oxime turned out to be superior to both acetone oxime as well as cyclopentanone oxime in terms of rate. If the reaction proceeds via tetrahedral intermediates **5 – 7** (Scheme 2), the results with different oximes suggest that the most likely candidates for the rate-determining step are either the first step (addition of H_2O) or the last step (expulsion of water and subsequent deprotonation). The faster rates obtained with β,β-disubstituted enals seemed to rule out the first possibility since the β substituents were unlikely to increase the rate of addition of H_2O to the oxime. These considerations suggested that the last step of the sequence (**7** - > **1**, Scheme 2) was the most likely candidate for the rate-determining step. However, the possibility that the reaction proceeds

via an alternative pathway, where the expulsion of the carbonyl compound and cyclization take place in the reverse order, could not be ruled out (Scheme 3).

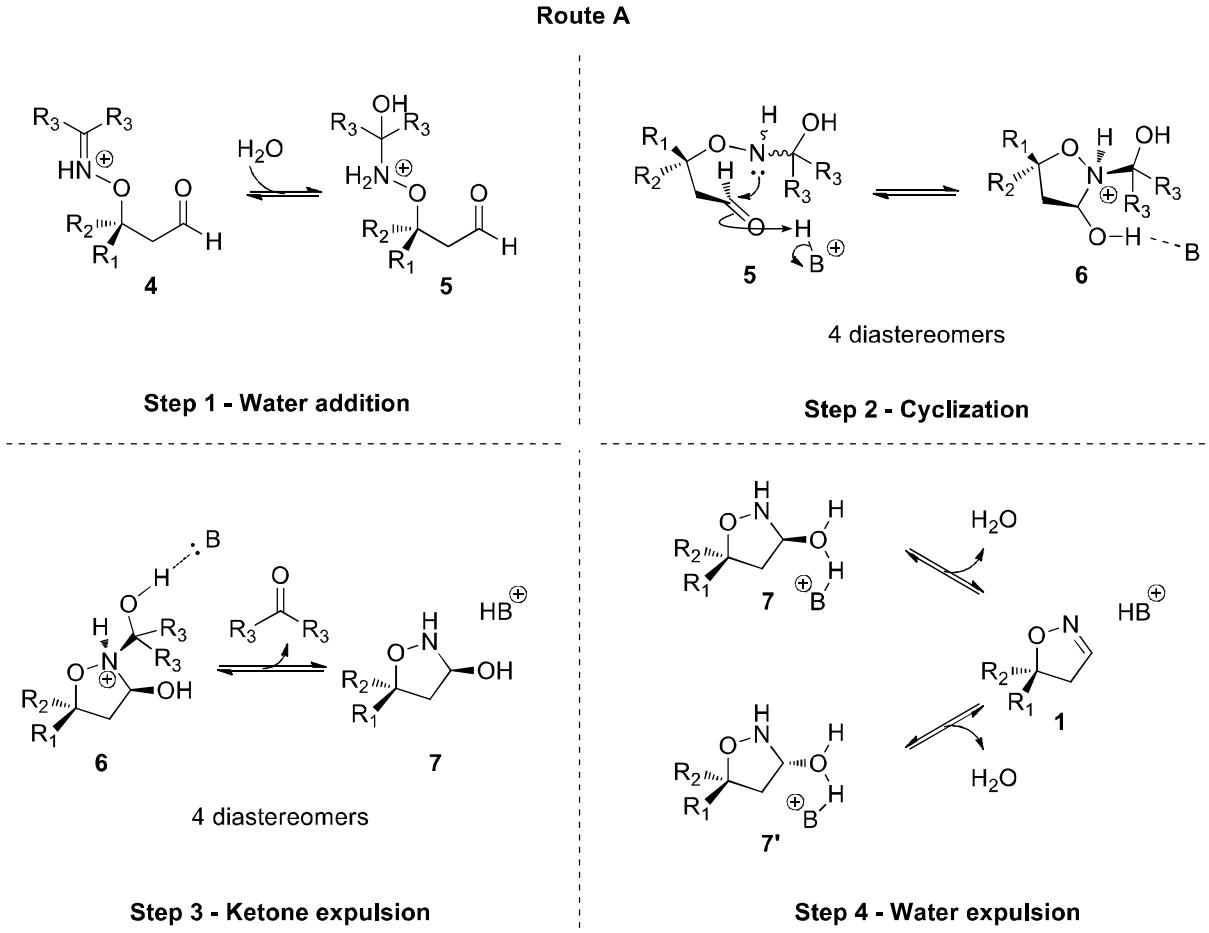

Scheme 2. Proposed reaction route for isoxazoline formation from conjugate addition product **4.**

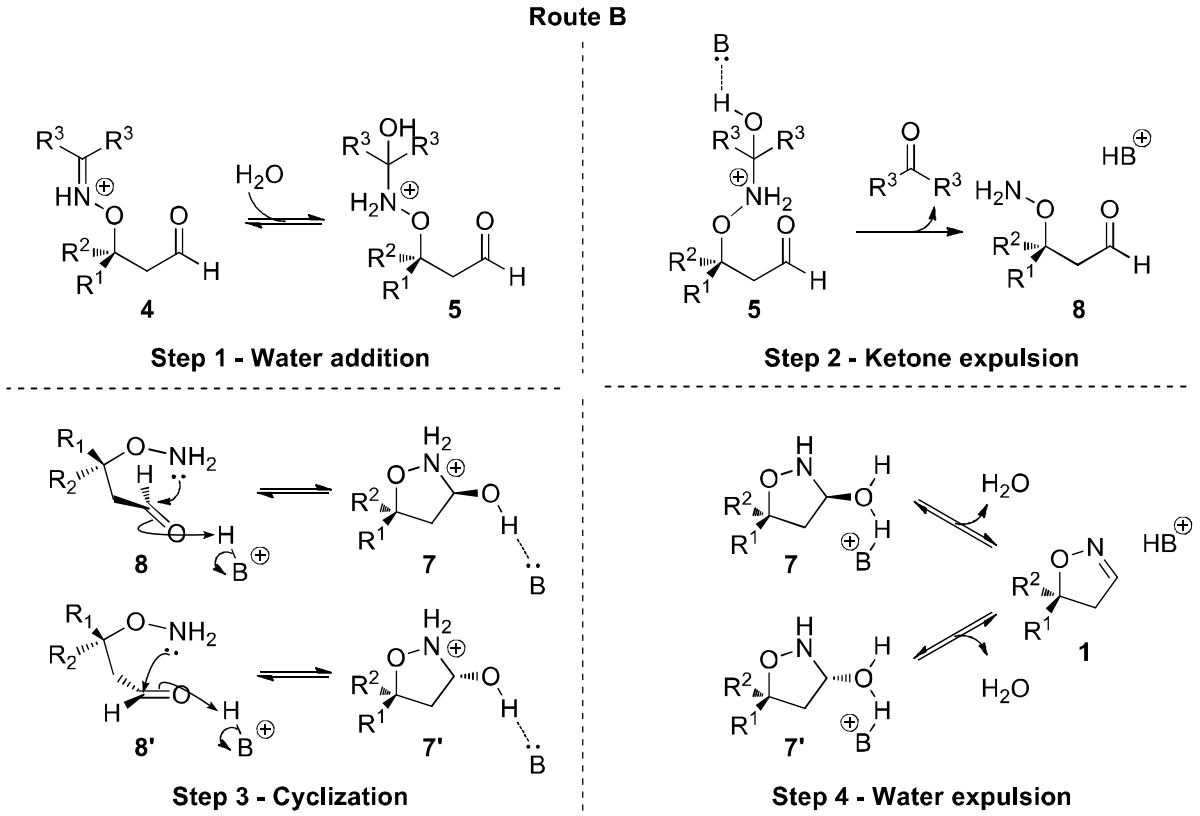

Scheme 3. Alternative reaction route for isoxazoline formation from conjugate addition product **4**.

If the reaction occurs via route A, the oxime transfer reaction is likely initiated by the water addition step in which the water molecule attacks the oxime group of the conjugate addition product (**4**). As the conjugate addition product is an observable intermediate (and thus reasonably stable), it can be assumed that the water addition step is slow without proper catalysis. Indeed, the importance of acid catalysis in the reversible addition of water to oximes has been shown in extensive mechanistic studies which were carried out in aqueous media and at various pH values.[2] The role of the acid catalysis in aqueous media has also been verified in computational studies.[3] Moreover, as mentioned above, the oxime transfer reaction takes place in the presence of an acid catalyst also in non-polar aprotic solvents. Based on these previous results, a reasonable first guess for the mechanism involves the reversible addition of water to the

conjugate addition product under acid catalysis. We are aware that the nucleophile could also be another species, such as another oxime, but here we consider water as the first choice of the nucleophile.

The addition of water should lead to a tetrahedral carbinolamine intermediate **5.** It is expected that the nitrogen in the carbinolamine is more nucleophilic than the nitrogen in the oxime species **4**, and thus, an acid catalyzed intramolecular 1,2-addition to aldehyde can proceed after the water addition step.[4]

Since the cyclization step yields a new carbinolamine **6** with additional stereocenters at nitrogen and C3, it is plausible that the cyclization step gives a mixture of diastereoisomers that lead to competitive reaction routes. Despite the effort, no diastereomeric intermediates **6** could be detected by ^{1}H NMR or trapped by silylation in previous experimental studies, indicating that the carbinolamine diastereomers are highly reactive intermediates within the reaction. As the carbinolamine stereocenters are lost after the water elimination step, the gathered experimental data provides no indication that one distereomeric route is favored over the others.[1b]

After the cyclization step, the expulsion of carbonyl compound can take place. This step is considered to be catalyzed by the conjugate base generated in the previous step. In addition to deprotonation of the forming oxonium ion, this step requires activation of the carbinolamine nitrogen by protonation. Sayer and co-workers found both of these factors to affect the rate of the reversible formation of tetrahedral carbinolamine products in acidic aqueous solutions.[4b] In addition, they concluded that the formation of a zwitterionic ammonium–alkoxide intermediate leads to a rapid collapse of the carbinolamine to an amine and a carbonyl species.

The final step of the oxime transfer reaction is the water expulsion that is comparable to the dehydration step of oxime formation reactions. Under aqueous and neutral conditions, the dehydration of the oxime is the rate determining step and the observed kinetic isotope effect is consistent with general acid catalysis.[4a] As a consequence, it is highly likely that the proton transfer or hydrogen bond activation of the hydroxyl group of the intermediate **7** catalyzes the water expulsion which yields a protonated isoxazoline species. Final deprotonation affords the desired 2-isoxazoline product.

In route B, the steps of route A are traced in reverse order. Therefore, the above reaction mechanism discussion is also applicable to the route B. However, if the cyclization step is reasonably fast, A will be more a potential route for the intramolecular oxime transfer reaction.[1b]

The purpose of the present study is to examine these reaction routes and steps in more detail and to find out the most plausible reaction mechanism for the intramolecular oxime transfer reaction by using DFT calculations. First, we shortly discuss our computational model systems. Second, we investigate the mechanism and the thermochemistry of the cyclization, carbonyl expulsion and water expulsion steps (steps 2-4 in schemes 2 and 3) of the oxime transfer reaction by means of the simple model systems (formaldehyde oxime models). Third, we study the whole reaction pathway by using more realistic system (acetone oxime model) with bulkier substituents and, finally, compare experimental and computational data.

Computational details

All calculations were performed employing the PBE0 hybrid exchange-correlation functional in conjunction with improved default triple-ζ valence polarized basis set, namely def2-TZVPP, in solution phase.[5,6] The presence of solvent was taken into account using the integral equation

formalism variant of the Polarizable Continuum Model (IEFPCM).[7] As a solvent, toluene was chosen, since the vast majority of the previous experimental work has been done in non-polar and aprotic solvents.

In order to locate the transition states, the potential energy hypersurface scans with respect to a selected internal reaction coordinate were carried out to get initial guesses for transition states, followed by full geometry optimizations. For optimized transition states, the intrinsic reaction coordinate (IRC) calculation was performed to acquire starting geometries for each reactants and products by following the reaction path along the transition vector to both directions.[8] Subsequent geometry optimizations were carried out for initial structures obtained from IRC calculations to find minimum structures for each intermediate. In all calculations, several different conformers were tested to locate the lowest energy minima and transition states on the potential energy hypersurface.

Frequency analyses were performed for all stationary points found to ensure that they correspond to either true minima (no imaginary frequencies) or first-order transition states (only one negative imaginary frequency). The thermochemical data were acquired at T = 298.15 K, P = 101.325 kPa (1 atm) using the ideal gas - rigid rotor - harmonic oscillator approximation as implemented in Gaussian09.[9]

To find out the rate determining states for the intramolecular oxime transfer reaction, we used the energetic span concept as defined by Kozuch and Shaik.[10] In this terminology, the efficiency of the catalytic cycle, i.e. the turnover frequency (TOF) is determined by one transition state and one intermediate which are called TOF-determining transition state (TDTS) and TOF-determining intermediate (TDI).

All calculations were performed with Gaussian 09 program,[9] whereas the visualizations of compounds were done with Mercury.[11]

Results and Discussion

Quantum chemical calculations were carried out for two different model systems, formaldehyde oxime ($R^1 = R^3 = H$, $R^2 = Me$) and acetone oxime ($R^1 = H$ $R^2 = R^3 = Me$), at PBE0/def2-TZVPP level of theory in solution phase.[5,6] Calculations were first carried out with the smaller formaldehyde oxime models since, to the best of our knowledge, no previous computational studies have been reported for the intramolecular oxime transfer reaction in the literature. Only a handful of similar computational and theoretical investigations exist but they have mainly concentrated on the hydrolysis and isomerization of oximes.[3] Hence, it was necessary first to get a preliminary picture from the oxime transfer reaction before quantum chemical calculations were performed for larger and more realistic acetone oxime models.

Although the compounds investigated in this study are already simplified if compared to the experimental setting, the model systems were further simplified in order to lower the computational cost of calculations by omitting the weakly coordinating anion, such as the diphenylphosphate anion. Moreover, it was important to include the solvent effect into to the calculation via integral equation formalism variant of the polarizable continuum model[7] since all experimental reactions take place in non-polar solutions and it has been showed in numerous studies that the presence of the solvent influences the reaction energy profile.[12] Toluene was chosen as the solvent for the solvation model.

In analogy to the experimental studies on oxime formation and hydrolysis,[2,4] the reaction pathway of the present oxime transfer reaction can be considered to include general acid or base

catalyzed steps which involve synchronous or rapid proton transfers. Since our previous experimental mechanistic studies on this reaction were carried out under moderately acidic conditions (oxoacids or their ammonium salts, see ref 1) methylammonium ion and its conjugate base methylamine were selected as the acid and base catalysts for the computational studies. In addition to this, the proposed intermediates have functionalities that can act as H-bond donors or acceptors. Therefore, it was crucial to use a quantum chemical method capable of describing hydrogen bonding and to ensure that the energy differences between diastereomeric routes do not arise solely from different hydrogen bond networks of optimized complexes.[13]

Reaction Mechanism: The computational examination of the oxime transfer reaction were started from route A and from the cyclization step using four formaldehyde oxime models **5a-5a'''**. Calculations reveal that the transition states $\mathbf{TS_{5a-6a}}$- $\mathbf{TS_{5a'''-6a'''}}$ involve a synchronized formation of a C-N single bond and a proton transfer from methylammonium to the aldehyde oxygen (Fig. 1, Fig. S1-S3). That is, the cyclization occurs in concerted manner. Following the transition vectors of transition states $\mathbf{TS_{5a-6a}}$-$\mathbf{TS_{5a'''-6a'''}}$ to forward direction lead to the closure of the five membered ring in each case and the formation of four diastereomers **6a-6a'''** with stereocenters at nitrogen, C3 and C5 (2-isoxazoline numbering).[14] In the product complex, methylamine is hydrogen bonded to all diastereomers in a similar manner.

The aldehyde expulsion step begins with the structural reorganization of hydrogen bonded complexes of **6a-6a'''**, giving four new complexes **6b-6b'''**, respectively, in which methylamine forms a new hydrogen bond with the hydroxyl group of the carbinolamine group (Fig. 1, Fig. S1-S3). This reorganization ensures that methylamine can act as a base catalyst in the aldehyde expulsion step. After the reorganization, the aldehyde expulsion step proceeds in concerted manner just like the cyclization step: transition states $\mathbf{TS_{6b-7a}}$-$\mathbf{TS_{6b'''-7a'''}}$ involve a proton transfer

from carbinolamine to methylamine in conjunction with C-N single bond breaking between the expulsing formaldehyde and ring system. As a consequence, four hydrogen bond complexes **7a-7a'''**are formed. Although the hydrogen bond complexes of **6b-6b'''** and **7a-7a'''** are quite identical, small variations can be seen in transition states ($\mathbf{TS_{6b\text{-}7a}}$ and $\mathbf{TS_{6b'\text{-}7a'}}$ vs. $\mathbf{TS_{6b''\text{-}7a''}}$ and $\mathbf{TS_{6b'''\text{-}7a'''}}$) due to the different orientation of the hydroxyl group of isoxazolidine ring (Fig. 1, Fig. S1-S3).

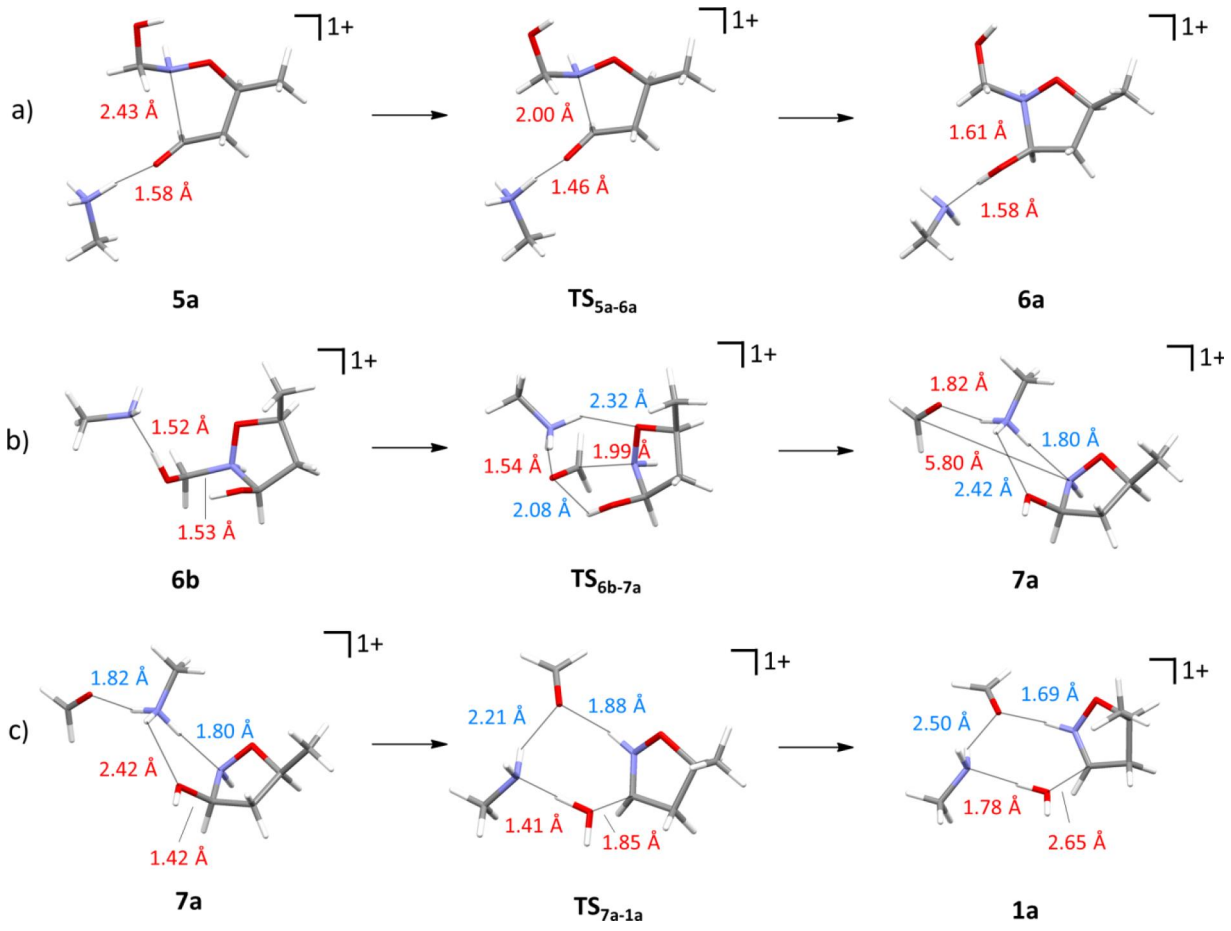

Figure 1. Optimized geometries of reagents, transitions states and products for the first diastereomer of formaldehyde oxime model: a) cyclization, b) aldehyde expulsion and c) water expulsion step. Color code: red = reaction coordinate and blue = hydrogen bond. Optimized geometries of three other diastereomers are presented in supporting information (Fig.S1-S3).

The close spatial proximity of methylammonium ion and the hydroxyl group of the oxime in hydrogen bond complexes **7a** and **7a'** enables the last step of the oxime transfer reaction (the water expulsion step) to proceed without significant reorganization of **7a** or **7a'**. However, **7a''** and **7a'''** have to undergo reorganization to **7b''** and **7b'''** prior to the water expulsion step can take place (Fig. 1 and Fig. S1-S3). This reorganization has also effect on the geometries of transition states $\mathbf{TS_{7b''\text{-}1a}}$ and $\mathbf{TS_{7b'''\text{-}1a}}$ which display dissimilar hydrogen bonded complexes than $\mathbf{TS_{7a\text{-}1a}}$ and $\mathbf{TS_{7a'\text{-}1a}}$. Despite the different hydrogen bond networks, the transition vectors of all transition states are connected to a proton transfer from methylammonium ion to the hydroxyl group of oxime and the breaking of O-C single bond of hydroxyl group. These processes are also evident from the structural changes (Fig. 1): for example, the length of O-C bond is 1.42 Å, 1.85 Å and 2.65 Å in **7a**, $\mathbf{TS_{7a\text{-}1a}}$, **1a**, respectively, indicating the clear elongation of O-C single bond during the reaction. IRC calculations for $\mathbf{TS_{7a\text{-}1a}}$-$\mathbf{TS_{7b'''\text{-}1a}}$ followed by geometry optimizations confirm that transition states lead to the desired reaction product **1a** of which a proton can be removed spontaneously in the presence of the base (see below discussion, Fig. S4, and Tab. S2).

For each step in the route B, the conformations of the starting complex and the product were optimized, and transition states searched. However, all potential energy surface (PES) scans with respect to the expulsion of the carbonyl compound from the intermediate **5** led to higher energy complexes. Also, no reasonable transition state could be found for this step. Thus, it is highly unlikely that the oxime transfer reaction takes place through the reaction pathway B, and, therefore, pathway B was excluded from further study.

Reaction energy: The Figure 2 shows computed Gibbs free energies for all formaldehyde oxime models. All acyclic intermediates, **5a-5a'''**, react with a methylammonium via a low lying transition state to give cyclic intermediates **6a-6a'''**, respectively, which are lower in energy than

the corresponding acyclic intermediates. This result indicates that the cyclization step of the reaction is exergonic and proceeds spontaneously. Even though the equilibrium of this step should be on the right side, it is feasible that the acyclic and cyclic intermediates are in a fast equilibrium due to their similar energies and small activation barriers between these two reactive species. Although the transitions states and products of the first and third diastereomers are slightly lower in energy than the corresponding species of the second and fourth diastereomers, results imply that all diastereomers **6a-6a'''** are accessible and the overall significance of the cyclization step to the oxime transfer reaction is minor.

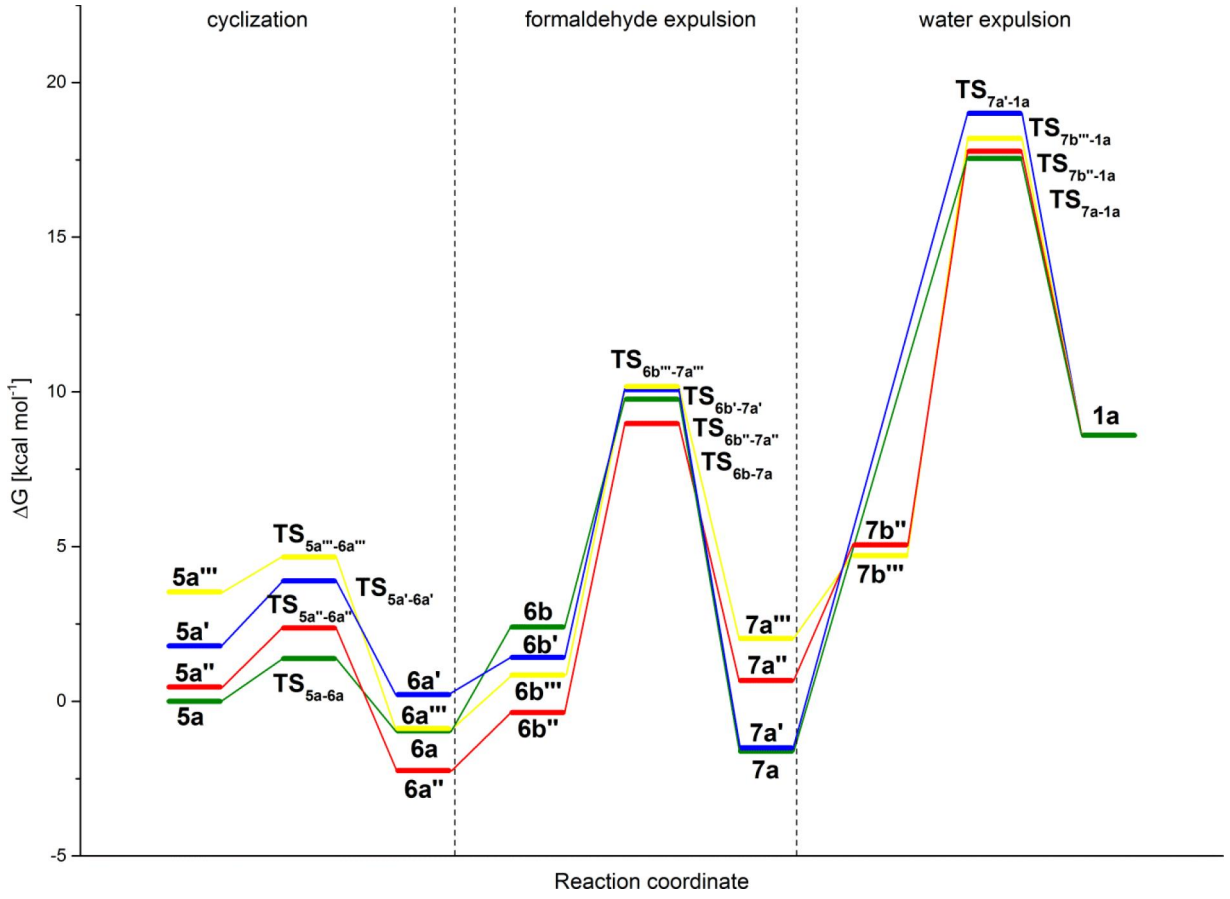

Figure 2. Calculated Gibbs free energies for formaldehyde oxime models: diastereomer 1 (green), diastereomer 2 (blue), diastereomer 3 (red) and diastereomer 4 (yellow). All values are scaled to Gibbs free energy of **5a** and they are also listed in Table S1.

According to the proposed mechanism and calculations, methylamine participates in the aldehyde expulsion step by general base catalysis and, thus, the expulsion of formaldehyde requires that methylamine coordinates to the proton of the formaldehyde carbinolamine. These changes in coordination (from **6a-6a'''** to **6b-6b'''**) are slightly unfavorable in regard to free energy (Fig. 2). The aldehyde expulsion step has a higher activation barrier than the cyclization step: the activation energies of diastereomers vary between 1.0 and 2.1 kcal mol^{-1} in the cyclization step, whereas in the aldehyde expulsion step they are in the range of 9.9-11.2 kcal mol^{-1}.[15] This result and the fact that the intermediates **7a-7a'''** are clearly lower in energy than transition states $\mathbf{TS_{7a\text{-}1a}}$-$\mathbf{TS_{7b'''\text{-}1a}}$ indicates that aldehyde expulsion step is not as reversible as the cyclization step.

As the experimental data suggested that the water expulsion step might be the rate determining step, we decided to study this step in more detail by calculating the Gibbs free energy of the reaction under different conditions. Firstly, the water expulsion step was studied by including the expulsed formaldehyde molecule in the complex in order to get a correct energy scaling for the whole reaction in case of all diastereomers. Secondly, for the first diastereomer series (**5a-1a**) additional calculations were made in which a number of hydrogen bonds within complex were varied and reaction conditions were changed from acidic to basic (for more details, see Fig. S4 in the SI).

It is evident from Figure 2 that the reorganization of the hydrogen bond complex from **7a''** (**7a'''**) to **7b''** (**7b'''**) changes the free energies of the complexes: **7b''** and **7b'''** are 4.4 and 2.7 kcal mol^{-1} higher in energy than **7a''** and **7a'''**, respectively. Hence, the reorganization is not

energetically favorable but necessary for the water elimination step to occur. The calculated transition states **$TS_{7a\text{-}1a}$-$TS_{7b'''\text{-}1a'''}$** are global energy maxima for formaldehyde oxime models, suggesting that the TS of the water expulsion step would be the TDTS in this case. As the stereocenters at nitrogen and carbon in position 3 are lost within the water expulsion step, the transition states lie almost in same free energy on the potential energy surface and lead to the protonated reaction product **1a** which is higher in energy than the corresponding starting materials. The energy of the protonated species drop significantly when the proton is removed from the ring system to afford the final isoxazoline product which is the global energy minima for whole reaction (see below).

The effect of the relative stereochemistry on the entire reaction pathway is small but nevertheless evident from the computations. The first (**5a-7a**) and the third (**5a''-7a''**) diastereomer series allow ~0.3-4.0 kcal mol^{-1}lower energies for the cyclization and aldehyde expulsion steps, whereas the starting complexes of the first and the second diastereomer series (**7a** and **7a'**) are ~2.0-4.0 kcal mol^{-1} lower in energy in the water expulsion step compared to the other two series. The similar hydrogen bond networks in the cyclization step (**5a-5a'''**, **6a-6a'''** and **$TS_{5a\text{-}6a}$-$TS_{5a'''\text{-}6a'''}$**) imply that the hydrogen bonding has little contribution to the energy differences in this step. On the contrary, the energy differences between intermediates **7a-7a'''** are affected to some degree by the H-bond networks as they cannot form identical complexes due to different configuration of functional groups.

In order to determine the importance of the number of hydrogen bonds in the complexes, the calculations for the water expulsion step were performed starting from singly (**7c**) and doubly (**7d**) hydrogen bonded intermediates. As expected, the doubly hydrogen bonded complex is stabilized by the additional H-bond (~4.0 kcal mol^{-1}) but it has an unfavorable effect, although

very small (~0.5 kcal mol^{-1}), on the transition state energy. The energy difference could be explained by a higher entropic cost relative to the singly H-bonded starting complex and the loss of stabilization due to the weakened H-bond.

As the oxime formation from hydroxylamine and carbonyl compounds is known to be pH sensitive in aqueous solutions[2a] and the oxime transfer step was highly dependent on the pK_{aH} of the amine catalyst, e.g. *N*-methylaniline versus pyrrolidine,[1b] we expected to see differences in the transition state energies in acidic and basic conditions. Thus, the calculations for the isoxazoline formation from carbinolamine were also performed in the presence of one equivalent of base (hydroxide ion without **7e** and with expulsed formaldehyde **7f** or methylamine **7g**). From these results, the effect of the acid catalyst on the transition state energy is clear. The activation energy of transition states $\mathbf{TS_{7a\text{-}1a}}$ is 19.2 kcal mol^{-1}, whereas the activation barrier is raised in the presence of hydroxide anion significantly higher: 28.2 and 31.4 kcal mol^{-1} for $\mathbf{TS_{7e\text{-}1d}}$ and $\mathbf{TS_{7f\text{-}1e}}$, respectively (Tab. S2). The effect of a neutral methylamine base is smaller, and it show similar activation energy (21.8 kcal mol^{-1}) for the water expulsion step. As such, the catalytic effect of the methylammonium ion survives buffered conditions (the presence of methylamine) but it is lost in the presence of a stronger base.

In summary, calculations for the simple formaldehyde oxime models confirm that the reaction pathways of intramolecular oxime transfer reaction contains general acid or base catalyzed equilibrium steps, which involve synchronous or rapid proton transfers. Based on the reaction energy data, the first two equilibrium steps of the intramolecular oxime transfer reaction can affect the overall reaction rate via the concentration of **7**. However, the water elimination step - that has the highest transition state and activation energy - most likely plays a more important role in the reaction. It should also be added that the intermediates and side products of each step

have the ability to form different kinds of hydrogen bonded complexes and small changes in these complexes can alter the reaction energy profile significantly.

Acetone oxime model system: The reaction mechanism of an intramolecular oxime transfer reaction was also investigated in case of more realistic systems (R^3= Me, acetone oxime) since this oxime was used in most of the experimental studies.[1,16] Furthermore, it was still unclear why the intermediate **4** is the only species of all intermediates which has been observed in experimental studies although computational studies for the formaldehyde oxime model (R^3 = H) suggests that the intermediate **7** might be observable in the reaction mixture due to the considerable activation barrier of the water expulsion step. To address the question whether the simplicity of the formaldehyde oxime model might have biased the results, calculations of acetone oxime model were carried out starting from the water addition step.

The results show that the water addition step likely takes place via a stepwise mechanism (Fig. 3). The first transition state $\mathbf{TS_{4i\text{-}4j}}$ involves two proton transfer reactions: from methyl ammonium ion to water and from water to nitrogen atom of the conjugate addition product **4i**. The second transition state $\mathbf{TS_{4j\text{-}5i}}$ contains also two simultaneous events: the attacking water molecule attaches to the electrophilic carbon atom of **4j** and donates the proton to methylamine at the same time. Even though two different transition states were located for the stepwise mechanism, no intermediate that is lower in energy than the transition state $\mathbf{TS_{4i\text{-}4j}}$ could be located between the two transition states $\mathbf{TS_{4i\text{-}4j}}$ and $\mathbf{TS_{4j\text{-}5i}}$. Hence, a concerted mechanism was also considered and characterized computationally. In the concerted mechanism, the attacking water molecule donates the proton to the conjugate addition product (Fig. 3, c). Thus, the methylammonium ion only carriers the positive charge through the step. The concerted reaction

pathway has a very high activation barrier (38.8 kcal mol^{-1} higher than $\mathbf{TS_{4i\text{-}5i}}$) indicating that the rapid stepwise mechanism is much more likely.

After the water addition step, the subsequent steps, *i.e.* the cyclization, expulsion of acetone, and expulsion of water, proceed in a similar manner for both, formaldehyde and acetone oxime, model systems and, thus, they are not discussed anymore in the case of acetone oxime model (optimized geometries of acetone oxime model are given in Fig. S5). Since our computational results for formaldehyde oxime models showed that the effect of different diastereomers on the overall reaction profile was relatively minor, for the last three steps of the reaction, we restrict our discussion only for the first diastereomer series (for **6i,** corresponding to 2*S**,3*R**,5S* relative stereochemistry) in case of acetone oxime model.

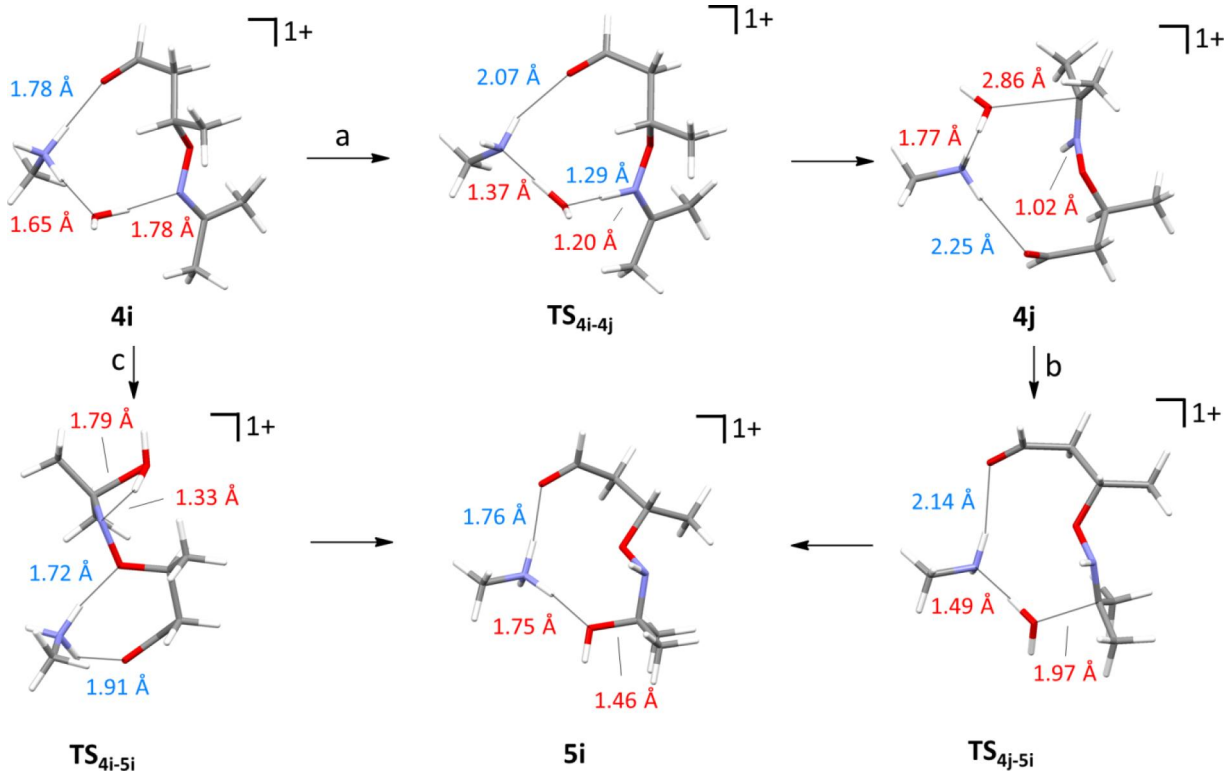

Figure 3. The calculated stepwise (a-b) and concerted mechanisms (c) of the water addition step for the acetone oxime model. Color code: red = reaction coordinate and blue = hydrogen bond.

As can be seen from the Figure 5, of all steps of the reaction, the water addition step has the highest transition state (**$TS_{4j\text{-}5i}$**) and it has also a high activation energy that is ca. 27 kcal mol^{-1}. This result is fully in line with previous computational studies where similar activation barriers were calculated for the addition of water to oximes.[3b] In addition, calculations indicate that the conjugate addition product **4i** is clearly lower in energy than the reaction product **5i** of the water addition step indicating that **4i** is thermodynamically stable. These computational findings readily explain the fact why the intermediate **4** can be detected experimentally and show that the water addition step is a good candidate for the rate-determining step in the intramolecular oxime transfer reaction.

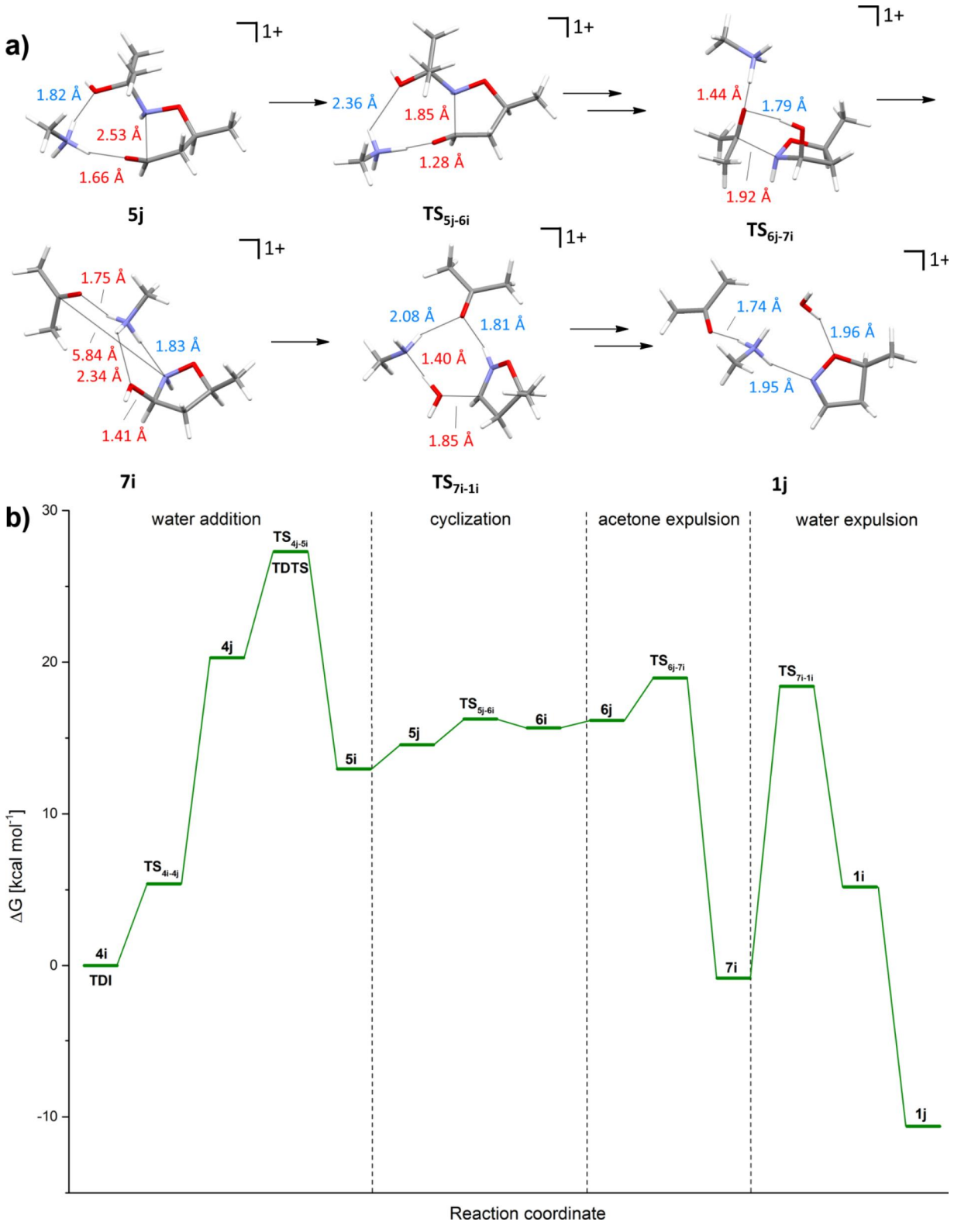

Figure 4. a) Optimized structures for **5j**, TS_{5j-6i}, TS_{6j-7i}, **7i**, TS_{7i-1i}, **1j** in last three steps (all optimized structures are given in supporting info, Fig. S5). b) Calculated Gibbs free energies for acetone oxime model (listed also in Tab. S3).

In the energetic span terminology, the TDI and TDTS are **4i** and $\mathbf{TS_{4j\text{-}5i}}$, respectively, indicating that the rate of the intramolecular oxime transfer reaction is mainly controlled by the water addition step. In our previous experimental studies, we suggested that the final water expulsion step would be the rate-determining step mainly on the basis of substituent effects observed with b,b-disubstituted enals. However, with simple b-monosubstituted enals (such as the model crotonaldehyde used in this study), the experimentally determined rates of the cyclization depended on the oxime structure in the order cyclohexanone oxime > acetone oxime > cyclopentanone oxime. This order corresponds roughly to the reactivity difference of the corresponding ketones to nucleophilic attack at carbonyl,[17] suggesting that at least with these oximes, the rate differences in the oxime transfer reaction might indeed be attributed to the rate of the nucleophilic attack.

Our calculations also indicate that the water expulsion step has a considerable activation barrier (~20.0 kcal mol^{-1}, Fig. 5). Although the computational model studied herein predicts the water addition step as the TDTS, it is conceivable that this picture could change with different substitution patterns in the enal, and both water addition as well as the water expulsion steps could contribute to the overall rate.[10,18,19] Moreover, the omitted counteranion could also influence on the reaction energy profile, although the relative energies of the intermediates and transition states are likely affected to a lesser extent than the absolute energies. The final product **1j** is much lower in energy (~10 kcal mol^{-1}) than the conjugate addition product indicating that the overall intramolecular oxime transfer reaction is clearly exergonic.

Conclusion

Density functional theory (PBE0/def2-TZVPP) calculations in conjunction with polarizable continuum model were used to assess the reaction mechanism of the intramolecular oxime transfer reaction and its reaction energy profile. Although the model compounds employed in the calculations were simplified from the experimental species, the computed activation barrier (27 kcal mol^{-1}) for the oxime transfer reaction is reasonable given the slow rate of the reaction. Moreover, calculations predicted that the formation and decomposition of tetrahedral intermediates, *i.e.* the addition of water to the oxime carbon, or the final expulsion of water to form the isoxazoline have higher barriers than the remaining steps. These predictions are in line with the experimental evidence obtained for this reaction. Hence, the pathway outlined in this study represents a highly likely pathway for the intramolecular oxime transfer reaction and the energy profiles obtained computationally are most likely valid depictions of the actual energy profiles. Nevertheless, since the counteranion was omitted from the model and different hydrogen bonding patterns of the intermediates affects the energies considerably, caution must be exercised in correlating the computed barriers with reaction rates.[20]

Acknowledgements

We thank Dr. Antti Pohjakallio and Dr. Heikki Tuononen for valuable discussions and input. Financial support has been provided by the University of Jyväskylä, the Academy of Finland and the Magnus Ehrnrooth Foundation.

References

[1] a) Pohjakallio, A.; Pihko, P. M. *Chem. Eur. J.* **2009**, *15*, 3960–3964. b) Pohjakallio, A.; Pihko, P. M.; Laitinen, U. M. *Chem. Eur. J*., **2010**, *16*, 11325–11339.

[2] a) Jencks, W. P. *J. Am. Chem. Soc.* **1959**, *81*, 475–481. b) More O'Ferrall, R. A.; O'Brien, D. *J. Phys. Org. Chem.* **2004**, *17*, 631–640.

[3] a) Yamaguchia, Y.; Yasutakeb, N.; Nagaokab, M. *J. Mol. Struc. (THEOCHEM)*, **2003**, *639*, 137–150. b) Nsikabaka, S.; Harb, W.; Ruiz-lópez, M. F. *J. Mol. Struc. (THEOCHEM)*, **2006**, *764*, 161–166. c) Takahashi, H.; Tanabe, K.; Aketa, M.; Kishi, R.; Furukawa, S.-I.; Nakano, M. *J. Chem. Phys.*, **2007**, *126*, 084508-084518. d) Ronchin, L.; Bortoluzzi, M.; Vavasori, A. *J. Mol. Struc. (THEOCHEM)*, **2008**, *858*, 46–51.

[4] a) Rosenberg, S.; Silver, S. M.; Sayer, J. M.; Jencks, W. P. *J. Am. Chem. Soc.* **1974**, *96*, 7986–7998. b) Sayer, J. M.; Pinsky, B.; Schonbrunn, A.; Washtien, W. *J. Am. Chem. Soc.* **1974**, *96*, 7998–8009.

[5] a) Perdew, J. P.; Burke, K.; Ernzerhof, M. *Phys. Rev. Lett*. **1996**, *77*, 3865–3868. b) Perdew, J. P.; Burke, K.; Ernzerhof, M. *Phys. Rev. Lett*. **1997**, *78*, 1396–1396. c) Perdew, J. P.; Ernzerhof, M.; Burke, K. *J. Chem. Phys*. **1996**, *105*, 9982–9985.

[6] Weigenda, F.; Ahlrichs, R. *Phys. Chem. Chem. Phys*. **2005**, *7*, 3297–3305.

[7] a) Miertuš, S.; Scrocco, E.; Tomasi, J. *Chem. Phys*. **1981**, *55*, 117-129. b) Miertuš, S.; Tomasi, J. *Chem. Phys*. **1982**, *65*, 239-245. c) Pascual-Ahuir, J. L.; Silla, E.; Tuñón, I. *J. Comp. Chem*. **1994**, *15*, 1127-1138. d) Cossi, M.; Barone, V.; Cammi, R.; Tomasi, J. *Chem. Phys. Lett*. **1996**, *255*, 327-335. (e) Barone, V.; Cossi, M.; Tomasi, J. *J. Chem. Phys*. **1997**, *107*, 3210-3221. f) Cancès, E.; Mennucci, B.; Tomasi, J. *J. Chem. Phys*. **1997**, *107*, 3032-3041. g) Mennucci, B.; Tomasi, J. *J. Chem. Phys*. **1997**, *106*, 5151-5158. h) Mennucci, B.; Cancès, E.; Tomasi, J. *J. Phys. Chem. B* **1997**, *101*, 10506-10517. i) Tomasi, J.; Mennucci, B.; Cancès, E. *J. Mol. Struct. (Theochem)*, **1999**, *464*, 211-226. j) Tomasi, J.; Mennucci, B.; Cammi R. *Chem. Rev*. **2005**, *105*, 2999-3093.

[8] a) Fukui, K. *Acc. Chem. Res*. **1981**, *14*, 363-368. b) Hratchian, H. P.; Schlegel, H. B. *J. Chem. Phys*. **2004**, *120*, 9918-9924. c) Hratchian, H. P.; Schlegel, H. B. *in Theory and Applications of Computational Chemistry: The First 40 Years*, Dykstra, C. E.; Frenking, G.; Kim, K. S.; Scuseria, G., Ed.; Elsevier: Amsterdam, 2005, pp 195-249. d) Hratchian, H. P.; Schlegel, H. B. *J. Chem. Theory and Comput*. **2005**, *1*, 61-69.

[9] Gaussian 09, Revision C.01, Frisch, M. J.; Trucks, G. W.; Schlegel, H. B.; Scuseria, G. E.; Robb, M. A.; Cheeseman, J. R.; Scalmani, G.; Barone, V.; Mennucci, B.; Petersson, G. A.; Nakatsuji, H.; Caricato, M.; Li, X.; Hratchian, H. P.; Izmaylov, A. F.; Bloino, J.; Zheng, G.; Sonnenberg, J. L.; Hada, M.; Ehara, M.; Toyota, K.; Fukuda, R.; Hasegawa, J.; Ishida, M.; Nakajima, T.; Honda, Y.; Kitao, O.; Nakai, H.; Vreven, T.; Montgomery, J. A., Jr.; Peralta, J. E.; Ogliaro, F.; Bearpark, M.; Heyd, J. J.; Brothers, E.; Kudin, K. N.; Staroverov, V. N.; Kobayashi, R.; Normand, J.; Raghavachari, K.; Rendell, A.; Burant, J. C.; Iyengar, S. S.; Tomasi, J.; Cossi, M.; Rega, N.; Millam, N. J.; Klene, M.; Knox, J. E.; Cross, J. B.; Bakken, V.; Adamo, C.; Jaramillo, J.; Gomperts, R.; Stratmann, R. E.; Yazyev, O.; Austin, A. J.; Cammi, R.; Pomelli, C.; Ochterski, J. W.; Martin, R. L.; Morokuma, K.; Zakrzewski, V. G.; Voth, G. A.; Salvador, P.; Dannenberg, J. J.; Dapprich, S.; Daniels, A. D.; Farkas, Ö.; Foresman, J. B.; Ortiz, J. V.; Cioslowski, J.; Fox, D. J. Gaussian, Inc., Wallingford CT, 2009.

[10] a) Kozuch, S.; Amatore, C.; Jutand, A.; Shaik, S. *Organometallics* **2005**, *24*, 2319-2330. b) Kozuch, S.; Shaik S. *Acc. Chem. Res.* **2011**, *44*, 101-110.

[11] Macrae, C. F.; Bruno, I. J.; Chisholm, J. A.; Edgington, P. R.; McCabe, P.; Pidcock, E.; Rodriguez-Monge, L.; Taylor, R.; van de Streek, J.; Wood, P. A. *J. Appl. Crystallogr*. **2008**, *41*, 466-470.

[12] For some examples, see: a) Ilieva, S.; Galabov, B.; Musaev, D. G.; Morokuma, K.; Schaefer, H. F. *J. Org. Chem*. **2003**, *68*, 1496-1502. b) Jin, L.; Wang, W.: Hua, D. Lü, J. *Phys. Chem. Chem. Phys*. **2013**, *15*, 9034-9042. c) Schreiner, E.; Nair, N. N.; Marx, D. *J. Am. Chem. Soc*. **2009**, *131*, 13668-13675. (d) Wang, Y. –N.; Topol, I. A.; Collins, J. R.; Burt, S. K. *J. Am. Chem. Soc*. **2003**, *125,* 13265-13273. d) Pasălić, H.; Aquino, A. L.; Tunega, D.; Haberhauer, G.; Gerzabek M. H.; Georg, H. C.; Moraes, T.; Coutinho, K.; Canuto, S.; Lischka, H. *J. Comput. Chem.* **2010**, *31*, 2046-2055. e) Kuznetsov, M. L.; Kukushkin, V. Y. *J. Org. Chem*. **2006**, *71*, 582-592. f) Carzía Ruano, J. L.; Clemente, F. R.; González Gutiérrez, L.; Gordillo, R.; Martín Castro, A. M.; Rodríguez Ramos, J. H. *J. Org. Chem*. **2002**, *67*, 2926-2933.

[13] PBE0 is able to describe hydrogen bond in good accuracy, for some examples, see: a) Zhao, Y.; Truhlar, D. G *J. Chem. Theory Comput*. **2005**, *1*, 415-432. b) Johnson, E. R.; DiLabio, G. A. *Chem. Phys. Lett.* **2006**, *419*, 333-339.

c) Santra, B.; Michaelides, A.; Scheffler, M. *J. Chem. Phys*. **2007**, *127*, 184104. d) Campo, J. M.; Gázquez, J. L.; Trickey, S. B.; Vela, A. *J. Chem. Phys*. **2012**, *136*, 104108.

[14] The diastereomers are assigned as follows: **6a** (first diastereomer series): (2*R**,3*R**,5*S**), **6a'** (second diastereomer series): (2*R**,3*R**,5*R**), **6a''** (third diastereomer series): (2*R**,3*S**,5*S**), **6a'''** (fourth diastereomer series): (2*R**,3*S**,5*R**).

[15] The free energies of **6a-6a'''** are used to calculate the activation energies of the aldehyde expulsion step as they are starting materials for the aldehyde expulsion step and are lower in energy than **6b-6b'''**.

[16] For some examples, see: a) Calzadilla, M.; Malpica, A.; Cordova, T. *J. Phys. Org. Chem*. **1999**, *12*, 708–712. b) Gajewski, J. J. *J. Am. Chem. Soc*. **1979**, *101*, 4393–4394. c) Yoo, H. Y.; Houk, K. N. *J. Am. Chem. Soc*. **1997**, *119*, 2877-2884. d) Tian, J.; Houk, K. N.; Klärner, F. G. *J. Phys. Chem. A* **1998**, *102*, 7662-7667.

[17] a) Finiels, A.; Geneste, P. *J. Org. Chem.* **1979**, *44*, 1577. For a discussion of the reactivity difference between cyclohexanones and cyclopentanones, see: b) Brown, H. C.; Brewster, J. H.; Shechter, H. *J. Am. Chem. Soc.* **1954**, *76*, 467-474.

[18] It has been proved that in multi-step reactions several steps/states play an important role to determine an overall reaction rate. For some examples, see: a) Murdoch, J. R. *J. Chem. Edu*. **1981**, *58*, 32-36. b) Fey, N. *Dalton Trans*. **2010**, *39*, 296-310. c) Sparta, M.; Børve, K. J.; Jensen, V. R. *J. Am. Chem. Soc*. **2007**, *129*, 8487-8499. d) Zuidema, E.; Escorihuela, L.; Eichelsheim, T.; Carbó, J. J.; Bo, C.; Kamer, P. C. J.; van Leeuwen, P. W. N. M. *Chem.–Eur. J.* **2008**, *14*, 1843–1853.

[19] It is also observed in earlier studies that the computational and experimental methods can predict different steps for the rate-determining step (see ref. 18d.)

[20] In addition with above discussion, it should also be noted, that the inclusion of the expulsed acetone in calculations lowers the free energy of $\mathbf{TS_{7i\text{-}1i}}$ considerably due to the hydrogen bonded network. If the free energy of the transition state is calculated without expulsed acetone and then scaled to fit reaction energy data, $\mathbf{TS_{7i\text{-}1i}}$ is 2.5 kcal mol^{-1} higher in energy.